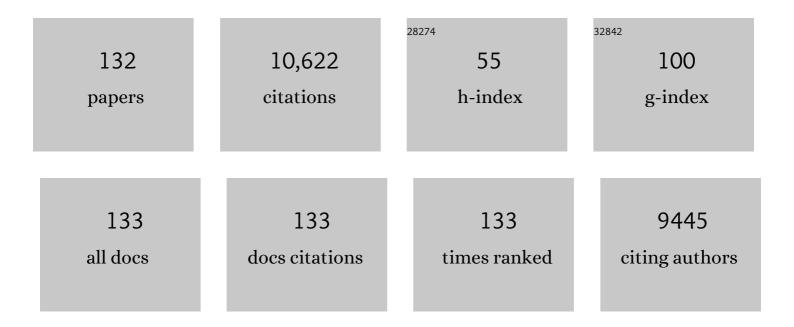
List of Publications by Year in descending order

Source: https://exaly.com/author-pdf/4846089/publications.pdf Version: 2024-02-01



WELKONG PANG

#	Article	IF	CITATIONS
1	Enhanced Sodium-Ion Battery Performance by Structural Phase Transition from Two-Dimensional Hexagonal-SnS ₂ to Orthorhombic-SnS. ACS Nano, 2014, 8, 8323-8333.	14.6	592
2	Understanding High-Energy-Density Sn4P3 Anodes for Potassium-Ion Batteries. Joule, 2018, 2, 1534-1547.	24.0	468
3	Graphitic Carbon Nanocage as a Stable and High Power Anode for Potassiumâ€ion Batteries. Advanced Energy Materials, 2018, 8, 1801149.	19.5	442
4	Boosting the Potassium Storage Performance of Alloyâ€Based Anode Materials via Electrolyte Salt Chemistry. Advanced Energy Materials, 2018, 8, 1703288.	19.5	382
5	Atomic Interface Engineering and Electricâ€Field Effect in Ultrathin Bi ₂ MoO ₆ Nanosheets for Superior Lithium Ion Storage. Advanced Materials, 2017, 29, 1700396.	21.0	343
6	Bio-inspired design of an <i>in situ</i> multifunctional polymeric solid–electrolyte interphase for Zn metal anode cycling at 30 mA cm ^{â^2} and 30 mA h cm ^{â^2} . Energy and Environmental Science, 2021, 14, 5947-5957.	30.8	289
7	Gallium-Doped Li ₇ La ₃ Zr ₂ O ₁₂ Garnet-Type Electrolytes with High Lithium-Ion Conductivity. ACS Applied Materials & Interfaces, 2017, 9, 1542-1552.	8.0	266
8	Toward Highâ€Performance Hybrid Znâ€Based Batteries via Deeply Understanding Their Mechanism and Using Electrolyte Additive. Advanced Functional Materials, 2019, 29, 1903605.	14.9	259
9	Enhanced Structural Stability of Nickel–Cobalt Hydroxide via Intrinsic Pillar Effect of Metaborate for High-Power and Long-Life Supercapacitor Electrodes. Nano Letters, 2017, 17, 429-436.	9.1	241
10	Tuning the Electrolyte Solvation Structure to Suppress Cathode Dissolution, Water Reactivity, and Zn Dendrite Growth in Zincâ€ion Batteries. Advanced Functional Materials, 2021, 31, 2104281.	14.9	225
11	An Intrinsically Nonâ€flammable Electrolyte for Highâ€Performance Potassium Batteries. Angewandte Chemie - International Edition, 2020, 59, 3638-3644.	13.8	211
12	Anion Vacancies Regulating Endows MoSSe with Fast and Stable Potassium Ion Storage. ACS Nano, 2019, 13, 11843-11852.	14.6	210
13	Boosting potassium-ion batteries by few-layered composite anodes prepared via solution-triggered one-step shear exfoliation. Nature Communications, 2018, 9, 3645.	12.8	204
14	Developing high-voltage spinel LiNi _{0.5} Mn _{1.5} O ₄ cathodes for high-energy-density lithium-ion batteries: current achievements and future prospects. Journal of Materials Chemistry A, 2020, 8, 15373-15398.	10.3	186
15	Plasmaâ€Induced Amorphous Shell and Deep Cation‣ite S Doping Endow TiO ₂ with Extraordinary Sodium Storage Performance. Advanced Materials, 2018, 30, e1801013.	21.0	180
16	Garnet-Type Fast Li-Ion Conductors with High Ionic Conductivities for All-Solid-State Batteries. ACS Applied Materials & Interfaces, 2017, 9, 12461-12468.	8.0	179
17	A new energy storage system: Rechargeable potassium-selenium battery. Nano Energy, 2017, 35, 36-43.	16.0	168
18	Li-Rich Layered Oxides and Their Practical Challenges: Recent Progress and Perspectives. Electrochemical Energy Reviews, 2019, 2, 277-311.	25.5	158

#	Article	IF	CITATIONS
19	Local Electric Field Facilitates High-Performance Li-Ion Batteries. ACS Nano, 2017, 11, 8519-8526.	14.6	155
20	Manipulating the Solvation Structure of Nonflammable Electrolyte and Interface to Enable Unprecedented Stability of Graphite Anodes beyond 2 Years for Safe Potassiumâ€lon Batteries. Advanced Materials, 2021, 33, e2006313.	21.0	155
21	Unraveling the effect of salt chemistry on long-durability high-phosphorus-concentration anode for potassium ion batteries. Nano Energy, 2018, 53, 967-974.	16.0	151
22	A Long Cycleâ€Life Highâ€Voltage Spinel Lithiumâ€lon Battery Electrode Achieved by Siteâ€Selective Doping. Angewandte Chemie - International Edition, 2020, 59, 10594-10602.	13.8	144
23	Heterostructure Manipulation <i>via in Situ</i> Localized Phase Transformation for High-Rate and Highly Durable Lithium Ion Storage. ACS Nano, 2018, 12, 10430-10438.	14.6	138
24	Hollow-Carbon-Templated Few-Layered V ₅ S ₈ Nanosheets Enabling Ultrafast Potassium Storage and Long-Term Cycling. ACS Nano, 2019, 13, 7939-7948.	14.6	136
25	Electrospun P2-type Na _{2/3} (Fe _{1/2} Mn _{1/2})O ₂ Hierarchical Nanofibers as Cathode Material for Sodium-Ion Batteries. ACS Applied Materials & Interfaces, 2014, 6, 8953-8958.	8.0	131
26	Interfacial Engineering of Nickel Boride/Metaborate and Its Effect on High Energy Density Asymmetric Supercapacitors. ACS Nano, 2019, 13, 9376-9385.	14.6	129
27	Insight of a Phase Compatible Surface Coating for Longâ€Durable Liâ€Rich Layered Oxide Cathode. Advanced Energy Materials, 2019, 9, 1901795.	19.5	129
28	Structural Insight into Layer Gliding and Lattice Distortion in Layered Manganese Oxide Electrodes for Potassiumâ€ion Batteries. Advanced Energy Materials, 2019, 9, 1900568.	19.5	125
29	Chromium Ion Pair Luminescence: A Strategy in Broadband Near-Infrared Light-Emitting Diode Design. Journal of the American Chemical Society, 2021, 143, 19058-19066.	13.7	125
30	An efficient multi-doping strategy to enhance Li-ion conductivity in the garnet-type solid electrolyte Li ₇ La ₃ Zr ₂ O ₁₂ . Journal of Materials Chemistry A, 2019, 7, 8589-8601.	10.3	124
31	Lithium Metal Electrode with Increased Air Stability and Robust Solid Electrolyte Interphase Realized by Silane Coupling Agent Modification. Advanced Materials, 2021, 33, e2008133.	21.0	122
32	Interplay between Electrochemistry and Phase Evolution of the P2-type Na _{<i>x</i>} (Fe _{1/2} Mn _{1/2})O ₂ Cathode for Use in Sodium-Ion Batteries. Chemistry of Materials, 2015, 27, 3150-3158.	6.7	121
33	Toward Understanding the Lithium Transport Mechanism in Garnet-type Solid Electrolytes: Li ⁺ Ion Exchanges and Their Mobility at Octahedral/Tetrahedral Sites. Chemistry of Materials, 2015, 27, 6650-6659.	6.7	107
34	Lithium Migration in Li ₄ Ti ₅ O ₁₂ Studied Using in Situ Neutron Powder Diffraction. Chemistry of Materials, 2014, 26, 2318-2326.	6.7	99
35	The Origin of Capacity Fade in the Li ₂ MnO ₃ ·Li <i>M</i> O ₂ (<i>M</i>) Tj Transmission X-ray Microscopy Study. Journal of the American Chemical Society, 2016, 138, 8824-8833.	ETQq1 1 13.7	0.784314 rg 96
36	Li ₂ TiSiO ₅ : a low potential and large capacity Ti-based anode material for Li-ion batteries. Energy and Environmental Science, 2017, 10, 1456-1464.	30.8	93

#	Article	IF	CITATIONS
37	Effects of Fluorine and Chromium Doping on the Performance of Lithium-Rich Li _{1+<i>x</i>} MO ₂ (M = Ni, Mn, Co) Positive Electrodes. Chemistry of Materials, 2017, 29, 10299-10311.	6.7	87
38	Super high-rate, long cycle life of europium-modified, carbon-coated, hierarchical mesoporous lithium-titanate anode materials for lithium ion batteries. Journal of Materials Chemistry A, 2016, 4, 9949-9957.	10.3	86
39	Dehydrationâ€Triggered Ionic Channel Engineering in Potassium Niobate for Li/Kâ€Ion Storage. Advanced Materials, 2020, 32, e2000380.	21.0	85
40	Facile synthesis of LiMn2O4 octahedral nanoparticles as cathode materials for high capacity lithium ion batteries with long cycle life. Journal of Power Sources, 2015, 278, 574-581.	7.8	83
41	Synergy of binders and electrolytes in enabling microsized alloy anodes for high performance potassium-ion batteries. Nano Energy, 2020, 77, 105118.	16.0	82
42	Na ₂ Ti ₆ O ₁₃ Nanorods with Dominant Large Interlayer Spacing Exposed Facet for Highâ€Performance Naâ€lon Batteries. Small, 2016, 12, 2991-2997.	10.0	78
43	Coupling Topological Insulator SnSb ₂ Te ₄ Nanodots with Highly Doped Graphene for Highâ€Rate Energy Storage. Advanced Materials, 2020, 32, e1905632.	21.0	78
44	Electron-Injection-Engineering Induced Phase Transition toward Stabilized 1T-MoS ₂ with Extraordinary Sodium Storage Performance. ACS Nano, 2021, 15, 8896-8906.	14.6	77
45	Constructing nitrided interfaces for stabilizing Li metal electrodes in liquid electrolytes. Chemical Science, 2021, 12, 8945-8966.	7.4	72
46	Voltammetric Enhancement of Li-Ion Conduction in Al-Doped Li _{7–<i>x</i>} La ₃ Zr ₂ O ₁₂ Solid Electrolyte. Journal of Physical Chemistry C, 2017, 121, 15565-15573.	3.1	71
47	In-situ neutron diffraction study of the simultaneous structural evolution of a LiNi0.5Mn1.5O4 cathode and a Li4Ti5O12 anode in a LiNi0.5Mn1.5O4 Li4Ti5O12 full cell. Journal of Power Sources, 2014, 246, 464-472.	7.8	70
48	Constructing the best symmetric full K-ion battery with the NASICON-type K3V2(PO4)3. Nano Energy, 2019, 60, 432-439.	16.0	67
49	Phase Evolution and Intermittent Disorder in Electrochemically Lithiated Graphite Determined Using in Operando Neutron Diffraction. Chemistry of Materials, 2020, 32, 2518-2531.	6.7	67
50	The Unique Structural Evolution of the O3â€Phase Na _{2/3} Fe _{2/3} Mn _{1/3} O ₂ during High Rate Charge/Discharge: A Sodium entred Perspective. Advanced Functional Materials, 2015, 25, 4994-5005.	14.9	66
51	Lanthanide doping induced electrochemical enhancement of Na ₂ Ti ₃ O ₇ anodes for sodium-ion batteries. Chemical Science, 2018, 9, 3421-3425.	7.4	66
52	Ultra-Broadband Phosphors Converted Near-Infrared Light Emitting Diode with Efficient Radiant Power for Spectroscopy Applications. ACS Photonics, 2019, 6, 3215-3224.	6.6	64
53	Structural Evolution and High-Voltage Structural Stability of Li(Ni _{<i>x</i>} Mn _{<i>y</i>} Co _{<i>z</i>})O ₂ Electrodes. Chemistry of Materials, 2019, 31, 376-386.	6.7	60
54	Inâ€Situ Powder Diffraction Studies of Electrode Materials in Rechargeable Batteries. ChemSusChem, 2015, 8, 2826-2853.	6.8	59

#	Article	IF	CITATIONS
55	<i>In Situ</i> Highâ€Temperature Diffraction Study of the Thermal Dissociation of Ti ₃ AlC ₂ in Vacuum. Journal of the American Ceramic Society, 2010, 93, 2871-2876.	3.8	58
56	Controlling of Structural Ordering and Rigidity of β-SiAlON:Eu through Chemical Cosubstitution to Approach Narrow-Band-Emission for Light-Emitting Diodes Application. Chemistry of Materials, 2017, 29, 6781-6792.	6.7	57
57	Self-Assembled Sandwich-like Vanadium Oxide/Graphene Mesoporous Composite as High-Capacity Anode Material for Lithium Ion Batteries. Inorganic Chemistry, 2015, 54, 11799-11806.	4.0	52
58	Understanding Rechargeable Battery Function Using In Operando Neutron Powder Diffraction. Advanced Materials, 2020, 32, e1904528.	21.0	52
59	Crystallographicâ€Siteâ€Specific Structural Engineering Enables Extraordinary Electrochemical Performance of Highâ€Voltage LiNi _{0.5} Mn _{1.5} O ₄ Spinel Cathodes for Lithiumâ€Ion Batteries. Advanced Materials, 2021, 33, e2101413.	21.0	52
60	In situ diffraction study of thermal decomposition in Maxthal Ti2AlC. Journal of Alloys and Compounds, 2011, 509, 172-176.	5.5	51
61	High rate capability core–shell lithium titanate@ceria nanosphere anode material synthesized by one-pot co-precipitation for lithium-ion batteries. Journal of Power Sources, 2014, 257, 280-285.	7.8	50
62	Designing a hybrid electrode toward high energy density with a staged Li ⁺ and PF ₆ ^{â^'} deintercalation/intercalation mechanism. Proceedings of the National Academy of Sciences of the United States of America, 2020, 117, 2815-2823.	7.1	50
63	Simple in situ synthesis of carbon-supported and nanosheet-assembled vanadium oxide for ultra-high rate anode and cathode materials of lithium ion batteries. Journal of Materials Chemistry A, 2016, 4, 13907-13915.	10.3	49
64	High-temperature thermal stability of Ti2AlN and Ti4AlN3: A comparative diffraction study. Journal of the European Ceramic Society, 2011, 31, 159-166.	5.7	46
65	Enhanced Rate-Capability and Cycling-Stability of 5 V SiO ₂ - and Polyimide-Coated Cation Ordered LiNi _{0.5} Mn _{1.5} O ₄ Lithium-Ion Battery Positive Electrodes. Journal of Physical Chemistry C, 2017, 121, 3680-3689.	3.1	45
66	Large-scale synthesis of ternary Sn5SbP3/C composite by ball milling for superior stable sodium-ion battery anode. Electrochimica Acta, 2017, 235, 107-113.	5.2	45
67	Eliminating Transition Metal Migration and Anionic Redox to Understand Voltage Hysteresis of Lithiumâ€Rich Layered Oxides. Advanced Energy Materials, 2020, 10, 1903634.	19.5	45
68	LiFePO ₄ Particles Embedded in Fast Bifunctional Conductor rGO&C@Li ₃ V ₂ (PO ₄) ₃ Nanosheets as Cathodes for Highâ€Performance Liâ€ion Hybrid Capacitors. Advanced Functional Materials, 2019, 29, 1807895.	14.9	42
69	Multi-Site Cation Control of Ultra-Broadband Near-Infrared Phosphors for Application in Light-Emitting Diodes. Inorganic Chemistry, 2020, 59, 15101-15110.	4.0	42
70	Polysulfide Filter and Dendrite Inhibitor: Highly Graphitized Wood Framework Inhibits Polysulfide Shuttle and Lithium Dendrites in Li–S Batteries. Advanced Functional Materials, 2021, 31, 2102458.	14.9	42
71	Ultrathin Fewâ€Layer GeP Nanosheets via Lithiationâ€Assisted Chemical Exfoliation and Their Application in Sodium Storage. Advanced Energy Materials, 2020, 10, 1903826.	19.5	41
72	Preparation and characterization of spinel LiNi0.5â^'xMgxMn1.5O4 cathode materials via spray pyrolysis method. Journal of Power Sources, 2013, 244, 35-42.	7.8	39

#	Article	IF	CITATIONS
73	In-situ Neutron Diffraction Study of a High Voltage Li(Ni0.42Mn0.42Co0.16)O2/Graphite Pouch Cell. Electrochimica Acta, 2015, 180, 234-240.	5.2	39
74	Insight into the improved cycling stability of sphere-nanorod-like micro-nanostructured high voltage spinel cathode for lithium-ion batteries. Nano Energy, 2019, 66, 104100.	16.0	38
75	Real-time powder diffraction studies of energy materials under non-equilibrium conditions. IUCrJ, 2017, 4, 540-554.	2.2	36
76	Evidence of Solid-Solution Reaction upon Lithium Insertion into Cryptomelane K _{0.25} Mn ₂ O ₄ Material. Journal of Physical Chemistry C, 2014, 118, 3976-3983.	3.1	35
77	Two-dimensional dysprosium-modified bamboo-slip-like lithium titanate with high-rate capability and long cycle life for lithium-ion batteries. Journal of Materials Chemistry A, 2016, 4, 17782-17790.	10.3	35
78	Accelerated Polysulfide Redox in Binderâ€Free Li ₂ S Cathodes Promises Highâ€Energyâ€Density Lithium–Sulfur Batteries. Advanced Energy Materials, 2021, 11, 2100957.	19.5	35
79	A custom battery for <i>operando</i> neutron powder diffraction studies of electrode structure. Journal of Applied Crystallography, 2015, 48, 280-290.	4.5	33
80	Comparison of the so-called CGR and NCR cathodes in commercial lithium-ion batteries using <i>in situ</i> neutron powder diffraction. Powder Diffraction, 2014, 29, S35-S39.	0.2	32
81	One-dimensional nanostructured design of Li _{1+x} (Mn _{1/3} Ni _{1/3} Fe _{1/3})O ₂ as a dual cathode for lithium-ion and sodium-ion batteries. Journal of Materials Chemistry A, 2015, 3, 250-257.	10.3	32
82	Comparison of thermal stability in <i>MAX</i> 211 and 312 phases. Journal of Physics: Conference Series, 2010, 251, 012025.	0.4	31
83	Solvothermal synthesis and electrochemical performance of hollow LiFePO4 nanoparticles. Journal of Alloys and Compounds, 2015, 640, 95-100.	5.5	31
84	Oxygen vacancy promising highly reversible phase transition in layered cathodes for sodium-ion batteries. Nano Research, 2021, 14, 4100-4106.	10.4	29
85	Synchrotron Xâ€Ray Absorption Spectroscopy and Electrochemical Study of Bi ₂ O ₂ Se Electrode for Lithiumâ€∤Potassiumâ€ion Storage. Advanced Energy Materials, 2021, 11, 2100185.	19.5	29
86	The storage degradation of an 18650 commercial cell studied using neutron powder diffraction. Journal of Power Sources, 2018, 374, 31-39.	7.8	28
87	Multiple Anionic Transition-Metal Oxycarbide for Better Lithium Storage and Facilitated Multielectron Reactions. ACS Nano, 2019, 13, 11665-11675.	14.6	28
88	Preparation and characterization of Cr-doped LiMnO2 cathode materials by Pechini's method for lithium ion batteries. Materials Chemistry and Physics, 2013, 139, 241-246.	4.0	27
89	In Situ Chelating Synthesis of Hierarchical LiNi _{1/3} Co _{1/3} Mn _{1/3} O ₂ Polyhedron Assemblies with Ultralong Cycle Life for Liâ€ion Batteries. Small, 2018, 14, e1704354.	10.0	27

 $\frac{1}{20}$ Electrochemistry and structure of the cobalt-free Li_{1+x}MO₂(M = Li, Ni, Mn,) Tj ETQq0 0 Qrg BT /Overlock 10 Tropped and the cobalt-free Li_{1+x}MO₂(M = Li, Ni, Mn,) Tj ETQq0 0 Qrg BT /Overlock 10 Tropped and the cobalt-free Li_{1+x}MO₂(M = Li, Ni, Mn,) Tj ETQq0 0 Qrg BT /Overlock 10 Tropped and the cobalt-free Li_{1+x}MO₂(M = Li, Ni, Mn,) Tj ETQq0 0 Qrg BT /Overlock 10 Tropped and the cobalt-free Li_{1+x}MO₂(M = Li, Ni, Mn,) Tj ETQq0 0 Qrg BT /Overlock 10 Tropped and the cobalt-free Li_{1+x}MO₂(M = Li, Ni, Mn,) Tj ETQq0 0 Qrg BT /Overlock 10 Tropped and the cobalt-free Li_{1+x}(M = Li, Ni, Mn,) Tj ETQq0 0 Qrg BT /Overlock 10 Tropped and the cobalt-free Li_{1+x}(M = Li, Ni, Mn,) Tj ETQq0 0 Qrg BT /Overlock 10 Tropped and the cobalt-free Li_{1+x}(M = Li, Ni, Mn,) Tj ETQq0 0 Qrg BT /Overlock 10 Tropped and the cobalt-free Li_{1+x}(M = Li, Ni, Mn,) Tj ETQq0 0 Qrg BT /Overlock 10 Tropped and the cobalt-free Li_{1+x}(M = Li, Ni, Mn,) Tj ETQq0 0 Qrg BT /Overlock 10 Tropped and the cobalt-free Li_{1+x}(M = Li, Ni, Mn,) Tj ETQq0 0 Qrg BT /Overlock 10 Tropped and the cobalt-free Li_{1+x}(M = Li, Ni, Mn,) Tj ETQq0 0 Qrg BT /Overlock 10 Tropped and the cobalt-free Li_{1+x}(M = Li, Ni, Mn,) Tj ETQq0 0 Qrg BT /Overlock 10 Tropped and the cobalt-free Li_{1+x}(M = Li, Ni, Mn,) Tj ETQq0 0 Qrg BT /Overlock 10 Tropped and the cobalt-free Li_{1+x}(M = Li, Ni, Mn,) Tj ETQq0 0 Qrg BT /Overlock 10 Tropped and the cobalt-free Li_{1+x}(M = Li, Ni, Mn,) Tj ETQq0 0 Qrg BT /Overlock 10 Tropped and the cobalt-free Li_{1+x}(M = Li, Ni, Mn,) Tj ETQq0 0 Qrg BT /Overlock 10 Tropped and the cobalt-free Li_{1+x}(M = Li, Ni, Mn,) Tj ETQq0 0 Qrg BT /Overlock 10 Tropped and the cobalt-free Li_{1+x}(M = Li) And the cobalt-free Li_{1+x}(M = Li) And the cobalt-free Li_{1+x}(M = Li) And the cobalt-fre

#	Article	IF	CITATIONS
91	Introducing 4 <i>s</i> –2 <i>p</i> Orbital Hybridization to Stabilize Spinel Oxide Cathodes for Lithiumâ€Ion Batteries. Angewandte Chemie - International Edition, 2022, 61, .	13.8	26
92	Oxidation characteristics of Ti3AlC2 over the temperature range 500–900°C. Materials Chemistry and Physics, 2009, 117, 384-389.	4.0	25
93	<i>In situ</i> incorporation of nanostructured antimony in an N-doped carbon matrix for advanced sodium-ion batteries. Journal of Materials Chemistry A, 2019, 7, 12842-12850.	10.3	25
94	In Situ Synchrotron Xâ€Ray Absorption Spectroscopy Studies of Anode Materials for Rechargeable Batteries. Batteries and Supercaps, 2021, 4, 1547-1566.	4.7	25
95	Doping with W6+ ions enhances the performance of TiNb2O7 as an anode material for lithium-ion batteries. Applied Surface Science, 2022, 573, 151517.	6.1	25
96	Crystallographic origin of cycle decay of the high-voltage LiNi _{0.5} Mn _{1.5} O ₄ spinel lithium-ion battery electrode. Physical Chemistry Chemical Physics, 2016, 18, 17183-17189.	2.8	24
97	Domination of Second-Sphere Shrinkage Effect To Improve Photoluminescence of Red Nitride Phosphors. Inorganic Chemistry, 2014, 53, 12822-12831.	4.0	23
98	Structural evolution of electrodes in the NCR and CGR cathode-containing commercial lithium-ion batteries cycled between 3.0 and 4.5 V: An operando neutron powder-diffraction study. Journal of Materials Research, 2015, 30, 373-380.	2.6	23
99	Engineering Unique Ball-In-Ball Structured (Ni _{0.33} Co _{0.67}) ₉ S ₈ @C Nanospheres for Advanced Sodium Storage. ACS Applied Materials & Interfaces, 2019, 11, 27805-27812.	8.0	22
100	In situ diffraction study on decomposition of Ti2AlN at 1500–1800°C in vacuum. Materials Science & Engineering A: Structural Materials: Properties, Microstructure and Processing, 2010, 528, 137-142.	5.6	20
101	Correlating cycling history with structural evolution in commercial 26650 batteries using in operando neutron powder diffraction. Journal of Power Sources, 2017, 343, 446-457.	7.8	20
102	A Long Cycleâ€Life Highâ€Voltage Spinel Lithiumâ€Ion Battery Electrode Achieved by Siteâ€Selective Doping. Angewandte Chemie, 2020, 132, 10681-10689.	2.0	20
103	Constructing Layered Nanostructures from Non‣ayered Sulfide Crystals via Surface Charge Manipulation Strategy. Advanced Functional Materials, 2021, 31, 2101676.	14.9	20
104	Effects of vanadium substitution on the cycling performance of olivine cathode materials. Journal of Power Sources, 2013, 241, 690-695.	7.8	18
105	Creating fast ion conducting composites via in-situ introduction of titanium as oxygen getter. Nano Energy, 2018, 49, 549-554.	16.0	18
106	Monitoring the phase evolution in LiCoO ₂ electrodes during battery cycles using inâ€situ neutron diffraction technique. Journal of the Chinese Chemical Society, 2020, 67, 344-352.	1.4	17
107	Hydrogen-Containing Na3HTi1–xMnxF8 Narrow-Band Phosphor for Light-Emitting Diodes. ACS Energy Letters, 2019, 4, 527-533.	17.4	16
108	An Intrinsically Nonâ€flammable Electrolyte for Highâ€Performance Potassium Batteries. Angewandte Chemie, 2020, 132, 3667-3673.	2.0	16

#	Article	IF	CITATIONS
109	In-situ diffraction studies on the crystallization and crystal growth in anodized TiO2 nanofibres. Materials Letters, 2012, 87, 150-152.	2.6	15
110	Capacity Enhancement of the Quenched Li-Ni-Mn-Co Oxide High-voltage Li-ion Battery Positive Electrode. Electrochimica Acta, 2017, 236, 10-17.	5.2	15
111	Synthesis of hierarchical mesoporous lithium nickel cobalt manganese oxide spheres with high rate capability for lithium-ion batteries. Applied Surface Science, 2018, 428, 1036-1045.	6.1	15
112	A New Lithiumâ€lon Conductor LiTaSiO ₅ : Theoretical Prediction, Materials Synthesis, and Ionic Conductivity. Advanced Functional Materials, 2019, 29, 1904232.	14.9	15
113	Thermal Stability of MAX Phases. Key Engineering Materials, 0, 617, 153-158.	0.4	14
114	Structure of the Li ₄ Ti ₅ O ₁₂ anode during charge-discharge cycling. Powder Diffraction, 2014, 29, S59-S63.	0.2	13
115	The use of deuterated ethyl acetate in highly concentrated electrolyte as a low-cost solvent for in situ neutron diffraction measurements of Li-ion battery electrodes. Electrochimica Acta, 2015, 174, 417-423.	5.2	13
116	Effect of AlF3-Coated Li4Ti5O12 on the Performance and Function of the LiNi0.5Mn1.5O4 Li4Ti5O12 Full Battery—An in-operando Neutron Powder Diffraction Study. Frontiers in Energy Research, 2018, 6,	2.3	12
117	Introducing 4 <i>s</i> –2 <i>p</i> Orbital Hybridization to Stabilize Spinel Oxide Cathodes for Lithiumâ€ion Batteries. Angewandte Chemie, 2022, 134, .	2.0	12
118	Understanding and improving the thermal stability of layered ternary carbides in ceramic matrix composites. , 2014, , 340-368.		11
119	A Robust Coinâ€Cell Design for In Situ Synchrotronâ€based Xâ€Ray Powder Diffraction Analysis of Battery Materials. Batteries and Supercaps, 2021, 4, 380-384.	4.7	11
120	In Operando Neutron Scattering Multiple‣cale Studies of Lithiumâ€ŀon Batteries. Small, 2022, 18, e2107491.	10.0	11
121	Characterisation of amorphous silica in air-oxidised Ti3SiC2 at 500–1000°C using secondary-ion mass spectrometry, nuclear magnetic resonance and transmission electron microscopy. Materials Chemistry and Physics, 2010, 121, 453-458.	4.0	8
122	Linking Macro- and Micro-structural Analysis with Luminescence Control in Oxynitride Phosphors for Light-Emitting Diodes. Chemistry of Materials, 2021, 33, 7897-7904.	6.7	8
123	Heterocarbides Reinforced Electrochemical Energy Storage. Small, 2019, 15, 1903652.	10.0	7
124	Sodium-ion battery anodes from carbon depositions. Electrochimica Acta, 2021, 379, 138109.	5.2	6
125	Synthesis and Properties of Recycled Paper-Nano-Clay-Reinforced Epoxy Eco-Composites. Key Engineering Materials, 2007, 334-335, 609-612.	0.4	5
126	Preparation and Characterization of Feâ€substituted Li ₃ V ₂ (PO ₄) ₃ Cathodes for Liâ€ion Batteries. Journal of the Chinese Chemical Society, 2012, 59, 1238-1243.	1.4	4

#	Article	IF	CITATIONS
127	In Situ Neutron Powder Diffraction Using Custom-made Lithium-ion Batteries. Journal of Visualized Experiments, 2014, , e52284.	0.3	4
128	Solid Electrolytes: A New Lithiumâ€lon Conductor LiTaSiO ₅ : Theoretical Prediction, Materials Synthesis, and Ionic Conductivity (Adv. Funct. Mater. 37/2019). Advanced Functional Materials, 2019, 29, 1970253.	14.9	4
129	Physical and Mechanical Properties of Mullite-Whisker Reinforced Alumina Composites. Key Engineering Materials, 2007, 334-335, 325-328.	0.4	3
130	Detection of Amorphous Silica in Air-Oxidized Ti ₃ SiC ₂ at 500–1000°C by NMR and SIMS. Key Engineering Materials, 0, 434-435, 169-172.	0.4	2
131	DIFFRACTION STUDY ON THE THERMAL STABILITY OF Ti[sub 3]SiC[sub 2]â^•TiCâ^•TiSi[sub 2] COMPOSITES IN VACUUM. AIP Conference Proceedings, 2010, , .	0.4	1
132	Mapping the Microstructure–Property Relationships in Cortical Bone. Key Engineering Materials, 2006, 309-311, 523-526.	0.4	0